

# Electric Field Patterning of Organic Nano-Architectures with Self-Assembled Molecular Fibers

*Volodymyr Duzhko,<sup>\*,†</sup> Jiangang Du,<sup>‡</sup> Christian A. Zorman,<sup>‡</sup> and Kenneth D. Singer<sup>†,‡</sup>*

Department of Physics and Department of Electrical Engineering and Computer Sciences,  
Case Western Reserve University, Cleveland, Ohio 44106, USA

## ABSTRACT

We discuss the manipulation of self-assembled semiconducting molecular nanofibers with electric fields of various geometries under photo-excitation. The nanofibers behave as electric dipoles, with the dipole moments arising from the spatial separation of photo-excited charge carriers in an external field. We utilized this interaction mechanism to align the nanofibers along electric field lines and position them between a specific pair of electrodes using a spatially inhomogeneous field. This approach enables high-precision and high-yield fabrication of advanced nanoarchitectures for organic molecular electronic, optoelectronic, and photonic devices.

---

\* Corresponding author. E-mail: [volodymyr.duzhko@case.edu](mailto:volodymyr.duzhko@case.edu).

† Department of Physics.

‡ Department of Electrical Engineering and Computer Sciences.

Self-assembled organic materials are being investigated for their potential in fabricating low-cost, environmental-friendly and energy-efficient devices. Self-assembly of organic molecules produces heterogeneous materials<sup>1</sup> and nanostructures<sup>2,3</sup> frequently built with atomic precision over extended length scales. Weak intermolecular interaction forces make the self-assembly process strongly responsive to external perturbations capable of producing novel functional architectures. Mimicking the architecture and functionality of objects in nature, research efforts are directed toward combining multiple functionalities in high precision, energy-efficient devices.

Self-assembled nanostructured objects, such as nanotubes,<sup>3</sup> nanofibers,<sup>2</sup> nanowires,<sup>4</sup> etc. promise nanoscale control of electronic, optoelectronic and photonic device architectures. While the long-term goal of self-assembled molecular electronics is to utilize hierarchical, non-covalent self-organization for building functional 3D architectures, integration of bottom-up and top-down fabrication approaches is proving fruitful. An important issue in bottom-up nanotechnology is the need to exert control over many length scales. Liquid-crystalline materials enhance the ability to span length scales due to the long-range nature of elastic forces along with the highly sensitive responses in the “soft” mesophases. Therefore, liquid crystalline phases and liquid-crystal templated crystallization are receiving considerable attention.

For an object of a one-dimensional geometry, precise placement and orientation is important in order to address the structure from the macroscopic world. Previous approaches to orienting specially functionalized nanowires utilized optical tweezers,<sup>5</sup> microfluidic channels<sup>6</sup> and Langmuir-Blodgett films,<sup>7</sup> magnetic<sup>8</sup> and electric fields.<sup>9,10</sup> In this paper, we discuss the interaction of self-assembled semiconducting nanofibers with electric fields of various geometries under photo-excitation. We show that the process arises from the interaction of an applied electric field with a photo-induced polarization due to the spatial

separation of photo-generated charge carriers. We demonstrate that the *orientation* and *position* of nanofibers can be precisely controlled over the large length scales as well as for individual nanofibers. As an illustration, we placed a single nanofiber from an extremely dilute solution between a selected pair of electrodes, and measured its dc conductivity. This simple and easily scalable approach does not require specially functionalized materials or complex instrumentation, and can be applied to a broad range of polarizable objects. It is expected to improve the fabrication of existing electronic nanodevices, such as nanowire-based field-effect-transistors,<sup>4</sup> and as well as to enable fabrication of more complex electronic, optoelectronic and photonic device architectures.

The fabrication of fibers of a phthalocyanine derivative, 2,3,9,10,16,17,23,24-octakis(octyloxy)-29H,31H-phthalocyanine ( $H_2Pc-OC_8$ ), have been previously described.<sup>2</sup> Briefly, the powder was dissolved in dodecane at elevated temperatures and then fibers were self-assembled upon cooling to room temperature, due to limited solubility. This procedure is similar to that described for perylene diimide derivatives.<sup>11</sup> The phthalocyanine derivatives are known for their large long-range hole mobility<sup>12</sup> and high extinction coefficient in the visible spectral range.<sup>13</sup> Figure 1 shows scanning electron microscopy (SEM) images of the fibers deposited from high- (B) or low-density (C) solutions, and an image of a single fiber (D) following deposition onto highly-oriented pyrolytic graphite (HOPG) and solvent evaporation. The fabrication procedure produces nanofibers in large quantities. The nanofiber diameter is distributed in the range of 150 nm to 500 nm. The observed uniform width along the fiber suggests a well-defined internal structure. We believe that the liquid crystalline phase promotes the uniformity of structure and allows, as previously shown, for control of fiber diameter.<sup>2</sup>

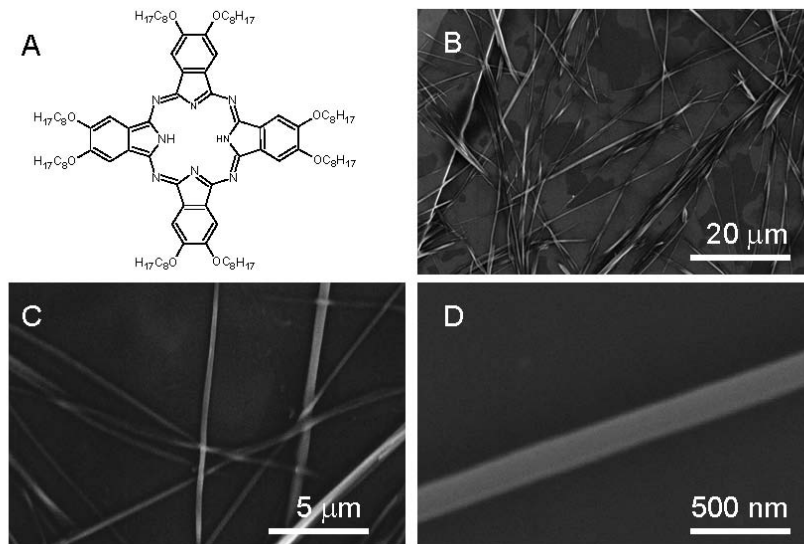


**Figure 1.** (A) Chemical structure of the H<sub>2</sub>Pc-OC<sub>8</sub> derivative. SEM images of nanofibers self-assembled from H<sub>2</sub>Pc-OC<sub>8</sub> in dodecane and deposited from concentrated (B) and dilute (C) solutions onto HOPG. (D) SEM image of a single H<sub>2</sub>Pc-OC<sub>8</sub> nanofiber with a width of ~170 nm.

Applied dc electric fields of various geometries were created by applying voltages ranging from 25V to 300 V between microelectrodes fabricated on insulating substrates. The microelectrodes consisted of patterned Au films on SiC-coated Si and Pyrex<sup>TM</sup> wafers. To fabricate the electrodes, the wafers were first coated with a 200 nm-thick, hydrophobic a-SiC:H film using a trimethylsilane-based, plasma enhanced chemical vapor deposition process detailed elsewhere.<sup>14</sup> The SiC films were deposited at 350°C and annealed at 450°C for 15 min in a N<sub>2</sub> atmosphere to relieve residual stress. Microelectrodes were then fabricated from an Au film deposited by DC magnetron sputtering and patterned using photoresist-based lift-off. A thin (few nm) Ti film was used to promote adhesion of the Au to the substrate. The thickness and width of the microelectrodes were 300 nm and 10 μm, respectively.

Fabrication and imaging of various nanofiber architectures in electric fields in two distinct geometries were carried out under an Olympus BX60 optical microscope. Both the incandescent microscope bulb and room light illumination were used when the deposition procedures were performed under illumination, otherwise the fibers were deposited in the dark and imaged after the solvent was completely evaporated. Evaporation of the solvent immobilized the nanofibers on the surface due to the van der Waals forces. SEM images were taken with a Hitachi S4500 SEM after the nanofibers were deposited onto a Pyrex<sup>TM</sup> surface and then sputtered with a thin Au film or, alternatively, merely deposited onto the freshly cleaved highly oriented pyrolytic graphite (HOPG, SPI supplies, grade 2). The I-V curves were measured with a Keithley 6517A electrometer.

Figures 2A-C show three patterns created after drop-casting nanofibers onto surfaces containing inhomogeneous electric fields of various geometries as generated by Au microelectrodes. Two distinct electric field geometries were utilized. In the first (Fig.2A), two parallel metal wires create a one-dimensional field in the plane between the wires. The electric field magnitude is shown in Figure 2D. The details of the electric field calculations are given elsewhere.<sup>15</sup> The nanofibers align themselves perpendicular to the micro-electrodes along the lines of electric field. In the second case (Fig.2B,C)), two “finger-tip” electrodes create an electric field that is inhomogeneous in both surface dimensions as shown in Figure 2E. Again, the nanofibers are aligned along the lines of electric field. In both Figures 2B and 2C, 200 V was applied during the fiber drop-casting. However, the electrode separation was smaller (50  $\mu\text{m}$ ) in Figure 2C versus 700  $\mu\text{m}$  in Figure 2B, yielding a much larger electric field in 2C versus 2B. In addition, the solution in Figure 2C was 100 times more dilute than in Figure 2B. Figure 2F shows electric field distribution normalized to the maximum field strength along the central line  $y = 0$  connecting the two electrodes. As can be seen in Figures

2 C and F, the nanofibers are attracted to the region of the strongest field and aligned along the field lines. The nanofibers aggregated upon solvent evaporation.

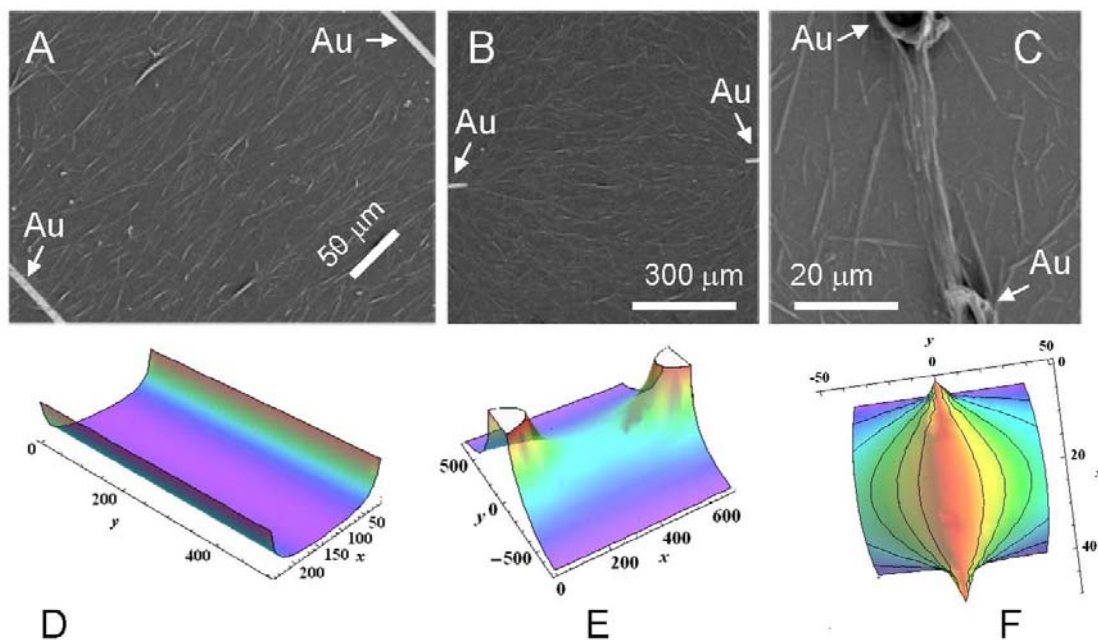


**Figure 2.** SEM images of  $H_2Pc-OC_8$  nanofibers drop-cast from dodecane onto the surface areas where the electric fields are inhomogeneous in one (A) or two (B,C) dimensions as generated by patterned Au microelectrodes as described in the text. The respective calculated geometries of electric fields (D,E) between the two Au electrodes of the two shapes are shown. Figure F shows electric field in the geometry as in Figure E, however the strength of electric field was normalized to the central line connecting the two electrodes ( $y=0$ ). The strength of electric field is given in arbitrary units and the lengths (x,y) are in microns.

The observed behavior of nanofibers in electric fields of various geometries can be described by the interaction of electric dipoles with electric field. In a homogeneous electric field  $E$ , an ideal dipole  $p$  (where  $p = ql$ ,  $q$  are charges on the opposite ends of a dipole, and  $l$

the separation distance) experiences a torque  $\vec{M} = [\vec{p}, \vec{E}]$  which tends to rotate the dipole along the lines of electric field to minimize its potential energy  $W = \vec{p} \cdot \vec{E}$ . In a spatially inhomogeneous field, different forces are exerted on the two oppositely charged ends of a dipole due to the field inhomogeneity. Then, the net force exerted on the dipole is given by  $\vec{F} = p \frac{\partial \vec{E}}{\partial l}$ , where the partial derivative is taken along the direction of a dipole moment. In any experiment, this force will attract the dipole to the regions of higher field.

Self-assembly of disc-like molecules in solution is governed by the  $\pi$ - $\pi$  interaction of their cores.<sup>3,16</sup> For stacked molecular packing, charge transport paths along the stacks, similar to hexagonal columnar mesophases of these discotic liquid crystalline materials, are expected to form. The photoconductivity of self-assembled hexabenzocoronene-trinitrofluorenone nanowires<sup>3</sup> and efficient charge transport in functionalized pentacene nanowires<sup>4</sup> have been recently demonstrated. Similarly, H<sub>2</sub>Pc-OC<sub>8</sub> nanofibers were found to transport charge (see discussion of Figure 3 below). We therefore consider H<sub>2</sub>Pc-OC<sub>8</sub> nanofibers to be semiconducting, *vide infra*, polarizable and possessing a limited number of charge carriers free to move under the influence of external field. Thermal generation and photo-excitation are the sources of free charge. Further, the electric field can both induce a polarization and redistribute any free charge. Both of these effects depend on the intrinsic material properties as well as on geometry of the self-assembled objects.

To understand the role of geometry for the induced polarization effects, the shape of a nanofiber can be approximated by a cylindrical geometry which is itself, similar to an ellipsoid. In an external field, the induced electric field in the dielectric polarization ellipsoid partially screens the external field due to induced surface charges. The net field is homogeneous and its magnitude is strongly shape-dependent.<sup>17</sup> For an elongated ellipsoid (cylinder) oriented along the lines of external field, the surface polarization charge, and

therefore the induced polarization field are small due to the limited surface area of the two ends of cylinder normal to the electric field lines. Thus, the interaction of polarization charge with the external electric field is weak due to the elongated geometry. This also leads to the condition that the thermally generated and photo-generated charge carriers experience the net electric field whose magnitude is nearly equal to the external field. Both of these effects favor photo-induced alignment and location by an inhomogeneous electric field.

In order to identify the dominant interaction mechanism, we performed two fabrication procedures, alignment under illumination and in the dark. In the dark, significantly smaller number of nanofibers was found in the area between the electrodes, and the fibers orientation was not as well defined compared with the case of alignment under illumination (see Figure S11 in the Supplemental Information). This indicates that both the dipole moments due to induced polarization and separation of thermally generated charge carriers, and therefore, potential interaction energy  $W$ , are significantly smaller than those due to the separation of photo-induced charge carriers. The spatial separation of photo-generated charges in the external field is therefore the dominant mechanism for the fiber-field interaction under illumination. We would also like to note that the induced polarization and separation of free charge carriers are expected to have different electric field frequency dependences. The free charge effects will be much smaller than polarization effects at higher frequency since the distance traveled by the free charges is shortened at higher frequencies.

The control over nanofiber orientation and location on a surface arising from their interaction with inhomogeneous electric fields (under illumination) enables fabrication of advanced device architectures using patterned microelectrodes. Illustration of this approach is shown in Figure 3B where an H<sub>2</sub>Pc-OC<sub>8</sub> nanofiber of ~ 200 nm in width has been deposited between two Au electrodes with a spacing of 7 μm. The electrodes were kept at a potential difference of 25 V during a fiber drop-casting. As discussed above, the photo-generated

charge in the nanofiber is separated in an external electric field creating an electric dipole. The interaction of this dipole with the inhomogeneous electric field orients and attracts the nanofiber along field lines which are freely moving in dilute solution. This localizes the fiber between the chosen electrodes and orients it along the field lines. Deposition of a single nanofiber (from dilute solution) into a specific electrode structure can be easily achieved with extremely high yield. The I-V characteristics of the nanofiber is shown in Figure 3C. The fact that a constant conductivity is observed shows the semiconducting nature of the nanofibers and its ability to transport charge. Further analysis of the conductivity magnitude most probably requires elucidation of contact phenomena.

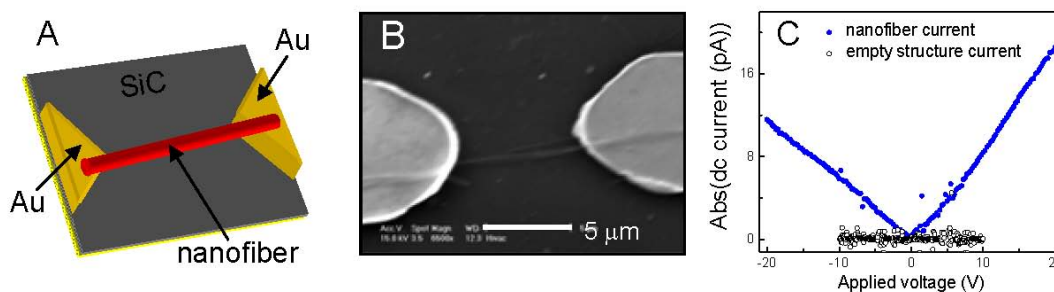


**Figure 3.** (A) Schematic image of a  $H_2Pc-OC_8$  nanofiber between two gold electrodes on a SiC surface. (B) Scanning electron microscopy image of the structure with nanofiber between the two Au electrodes and (C) current-voltage characteristic of the nanofiber.

In conclusion, we discussed the interaction of self-assembled semiconducting organic nanofibers with an applied electric field, and demonstrated that the most robust effect depends on photo-generated charge. Utilizing different geometries of inhomogeneous electric fields created by the patterning of micro-electrodes, we have achieved precise control over the orientation and position of organic semiconducting nanofibers. This approach is expected

to be applicable to any semiconducting nanowire, enabling both high yield and fine control over the fabrication of existing organic nanowire-based devices, as well as for the fabrication of more advanced device architectures.

**Supporting Information available.** Details of electric field calculations for various experimental geometries of electrodes and optical microscopy images comparing the phthalocyanine fibers deposition in the electric field under illumination or in the dark. This material is free of charge via the Internet at <http://pubs.acs.org>.

## References

- (1) Percec, V.; Glodde, M.; Miura, T.K.; Shiyonovskaya, I.; Singer, K.D.; Balagurusamy, V.S.K.; Heiney, P.A.; Schnell, I.; Rapp, A.; Spiess, H.-W.; Hudson, S.D.; and Duan, H. *Nature* **2002**, 417, 384.
- (2) Duzhko, V.; Singer, K.D. *J. Phys. Chem. C* **2007**, 111, 27.
- (3) Yamamoto, Y.; Fukushima, T.; Suna, Y.; Ishii, N.; Saeki, A.; Seki, S.; Tagawa, S.; Taniguchi, M.; Kawai, T.; Aida, T. *Science* **2006**, 314, 1761.
- (4) Briseno, A.L.; Mannsfeld, S.C.B.; Lu, X.; Xiong, Y.; Jenekhe, S.A.; Bao, Z.; and Xia, Y. *Nano Lett.* **2007**, 7, 668.
- (5) Dufresne, E.R.; Grier, D.G. *Rev. Sci. Instrum.* **1998**, 69, 1974.
- (6) Huang, Y.; Duan, X.; Wei, Q.; Lieber, C.M. *Science* **2001**, 291, 630.
- (7) Whang, D.; Jin, S.; Wu, Y.; and Lieber, C.M. *Nano Lett.* **2003**, 1255, 3.
- (8) Tanase, M.; Silevitch, D.M.; Hultgren, A.; Bauer, L.A.; Searson, P.C.; Meyer, G.J.; Reich, D.H. *J. Appl. Phys.* **2002**, 91, 8549.

- 
- (9) Smith, P.A.; Nordquist, C.D.; Jackson, T.N.; Mayer, T.S.; Martin, B.R.; Mbindyo, J.; Mallouk, T.E. *Appl. Phys. Lett.* **2000**, *77*, 1399.
- (10) Duan, X.; Huang, Y.; Cui, Y.; Wang, J.; and Lieber, C.M. *Nature* **2001**, *409*, 67.
- (11) Balakrishnan, K.; Datar, A.; Zhang, W.; Yang, X.; Naddo, T.; Huang, J.; Zuo, J.; Yen, M.; Moore, J.S.; Zang, L. *J. Am. Chem. Soc.* **2006**, *128*, 6576.
- (12) Iino, H.; Hanna, J.-I.; Bushby, R.J.; Movaghar, B.; Whitaker, B.J.; Cook, M.J. *Appl. Phys. Lett.* **2005**, *87*, 132102.
- (13) McKeown, N.B. *Phthalocyanine Materials: Synthesis, Structure and Function*; Cambridge University Press: Cambridge, 1998.
- (14) Du, J.; Singh, N.; Summers J.; and Zorman, C.A. *Mat. Res. Soc. Symp. Proc.* **2006**, *919*, 283.
- (15) See supporting information for calculations of electric fields in various experimental geometries.
- (16) Wu, J.; Fechtenkötter, A.; Gauss, J.; Watson, M.D.; Kastler, M.; Fechtenkötter, C.; Wagner, M.; and Müllen, K. *J. Am. Chem. Soc.* **2004**, *126*, 11311.
- (17) Landau L.D.; Lifshitz E.M. *Course of Theoretical Physics: Electrodynamics of continuous media*; Nauka: Moscow, 1981.

SYNOPSIS TOC

